



AQUEDUCT WATER STRESS PROJECTIONS: DECADAL PROJECTIONS OF WATER SUPPLY AND DEMAND USING CMIP5 GCMs

MATT LUCK, MATT LANDIS, AND FRANCIS GASSERT

EXECUTIVE SUMMARY

Climate change, global economic development, and population growth will alter the availability of and competition for water around the world. This analysis complements climate projections by giving information on future water availability that is relevant for decadal-scale planning, adaptation, and investment.

This document details the methodology used to produce global estimates of water stress, water demand, water supply, and seasonal variability for three 21-year periods centered on 2020, 2030, and 2040. Projections of climate variables were driven primarily by general circulation models from the Coupled Model Intercomparison Project (CMIP) Phase 5 project, and socioeconomic variables were based on the Shared Socioeconomic Pathways database from the International Institute for Applied Systems Analysis. All data are available at wri.org/aqueduct.

Overall results show rapid increases in water stress across many regions including the Mediterranean, the Middle East, the North American West, eastern Australia, western Asia, northern China, and Chile (Figure 1). Changes in water demand, driven by socioeconomic growth, are more dominant than changes in water supply, driven by climate. These results raise three points:

- Understanding growth in demand is at least as important as understanding changes in supply.
- Water managers may have the opportunity to avoid the majority of water stress increases through improved water demand management.
- In many areas, decisionmakers must be prepared for a wide range of possible outcomes.

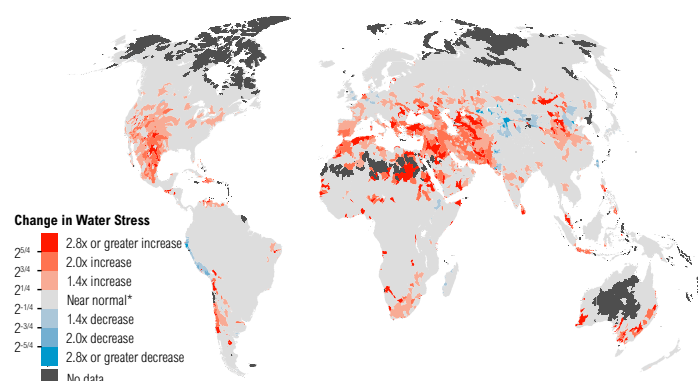
CONTENTS

1. Executive Summary.....	1
2. Background.....	2
3. Water supply.....	2
4. Water withdrawals.....	3
5. Indicators.....	8
6. Discussion.....	11
Endnotes.....	12
Appendix.....	14

Technical notes document the research or analytical methodology underpinning a publication, interactive application, or tool.

Suggested Citation: Luck, M., M. Landis, F. Gassert. 2015. "Aqueduct Water Stress Projections: Decadal Projections of Water Supply and Demand Using CMIP5 GCMs." Technical Note. Washington, D.C.: World Resources Institute. Available online at: wri.org/publication/aqueduct-water-stress-projections.

Figure 1 | Projected Change in Water Stress from Baseline (1950–2010) to Future (2030–50) under Business-as-Usual Scenario RCP8.5 SSP2



*Regions that increase in stress but remain at low stress levels (<0.1) and regions that decrease in stress but remain at extremely high stress levels (>0.8) are shown as “near normal.”

Box 1 | Scenarios

The scenarios in this report are based on a combination of projected water supply based on change in climate factors and water demand based on change in socioeconomic drivers.

REPRESENTATIVE CONCENTRATION PATHWAYS (RCPs) are scenarios of the increase in radiative forcing through 2100. These drive the climate factors in the General Circulation Models.

- **RCP8.5** is a “business-as-usual” scenario of relatively unconstrained emissions. Temperatures increase 2.6–4.8°C by 2100 relative to 1986–2005 levels.
- **RCP4.5** represents a “cautiously optimistic” scenario. Temperatures rise 1.1–2.6°C by 2100.

SHARED SOCIOECONOMIC PATHWAYS (SSPs) are scenarios of socioeconomic drivers.

- **SSP2** is a “business-as-usual” scenario.
- **SSP3** is a “pessimistic” scenario with higher population growth, lower GDP growth, and a lower rate of urbanization.

In section 5, three combinations of climate and socioeconomic scenarios are introduced: RCP4.5/SSP2, RCP8.5/SSP2, and RCP8.5/SSP3.

See Appendix for more information on the scenarios.

Many regions may also be subject to slight increases in seasonal variability in water supply within the coming decades implying higher probability of droughts or flooding. These changes could be partially mitigated by rapid global reduction in carbon emissions.

2. BACKGROUND

Both private and public sectors see the need to plan for potential changes in water availability caused by climate change and economic development.¹ While significant effort has been made to develop long-term projections of changes in water availability caused by climate change,² these projections are often for time periods too far in the future to be salient to decisionmakers.

With the goal of producing information for decadal-scale planning, adaptation, and investment, this analysis models potential changes in future demand and supply of water over the next three decades. Specifically, we focus on three aspects of water availability that are likely to change in the coming decades: the competition for water resources (often called water stress), total water supply (average annual flow), and the variability of water supply.

Globally we estimate indicators of water demand (withdrawal and consumptive use), water supply, water stress (the ratio of water withdrawal to supply), and intra-annual (seasonal) variability for the periods centered on 2020, 2030, and 2040 for each of two climate scenarios (RCP4.5 and RCP8.5) and two shared socioeconomic pathways (SSP2 and SSP3) (Box 1). We derived estimates from general circulation models (GCMs) from the Coupled Model Intercomparison Project Phase 5 (CMIP5)³ and mixed-effects regression models based on projected socioeconomic variables from the International Institute for Applied Systems Analysis (IIASA)’s Shared Socioeconomic Pathways (SSP) database.⁴ All indicators were resampled to a sub-basin scale to facilitate hydrological routing. Sections 3 and 4 describe methods for projection of water supply and water withdrawals, respectively. Section 5 describes indicator computation and results.

3. WATER SUPPLY

We computed water supply from runoff values extracted from an ensemble of CMIP5 GCMs.⁵ Six GCMs representing a broad lineage of models from geographically and methodologically diverse modeling centers, were selected based on their availability of required data for the RCP4.5 and RCP8.5 scenarios, and their ability to reproduce the

mean and standard deviation of historical runoff (see section A2 of Appendix). Several GCMs had results for multiple ensemble members available, for a total of 30 members across the two climate scenarios (13 for RCP4.5 and 17 for RCP8.5).

3.1. Bias Correction

Since GCM variables may systematically deviate from historical observations over their multicentury simulation period, we bias-corrected GCM output, specifically annual runoff for annual water supply indicators, annual irrigation consumptive use for annual water demand, and monthly runoff for the seasonal variability indicator. Bias-correction was performed via quantile-quantile mapping, also known as cumulative distribution function (CDF) matching following Mason.⁶ GCM output was matched to historical data from the Global Land Data Assimilation System Version 2 (GLDAS-2).⁷

To correct GCM output, we fit generalized extreme value (GEV) distributions⁸ separately for each pixel over the historical period data (1950–2005) for each GCM run and the corresponding GLDAS-2 output. We then corrected the GCM values by matching distributions (Figure 2).

3.2. Total and Available Blue Water

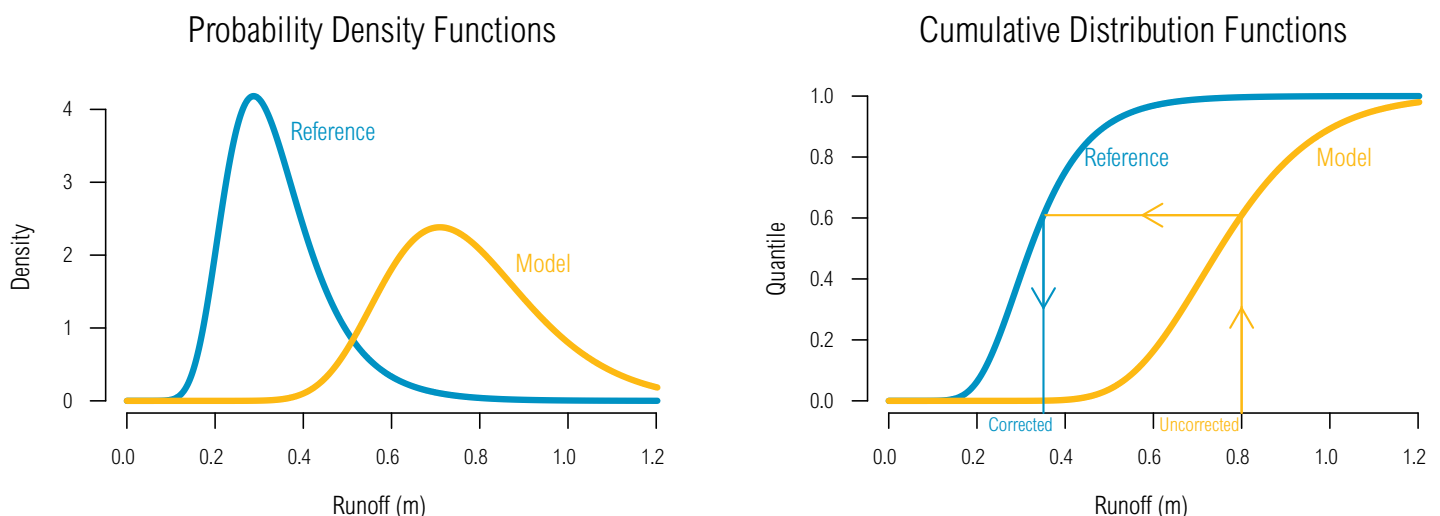
Bias-corrected runoff values were then resampled to 1 km × 1 km and summed into hydrological catchments to allow for the downstream flow-accumulation of water in rivers. The runoff data did not extend exactly to the coast in some areas, so the edges of the runoff data were expanded using focal fill with the mean of the surrounding cells to fill any incomplete catchments. From this we used a sparse catchment-to-catchment flow accumulation approach to compute two estimates of water supply following Gassert et al.:⁹ *total blue water* (*Bt*), which is flow-accumulated runoff, and *available blue water* (*Ba*), which accounts for upstream consumptive use. We calculated flow annually ignoring instream storage or retention.

4. WATER WITHDRAWALS

Water *withdrawals* and *consumptive* use were modeled from the projected size, wealth, and other characteristics of countries, for each of three sectors as defined by the Food and Agriculture Organization of the United Nations (FAO): agriculture, industry, and domestic.¹⁰

For all three sectors, we projected withdrawals (or irrigated area and irrigation efficiency in the case of the agriculture sector) with country-level regressions based on historical estimates of withdrawals. Since future scenarios were available for only three meaningful variables for each SSP (GDP, population, and urbanization),¹¹ regres-

Figure 2 | Bias Correction of Modeled Variables Using Quantile-Quantile Matching



The left panel shows the generalized extreme value distributions as probability density functions, where the blue curve is the reference distribution and the orange curve is the modeled distribution. The right panel demonstrates the use of the corresponding cumulative distribution functions to translate the value 0.8 to 0.34.

sion independent variables were limited to these three, as well as interactions and static variables such as baseline (2010) water stress (Table 1). Regression specifications are described in the following sections.

4.1. Irrigation Withdrawals

Agricultural withdrawals are by far the largest withdrawals. We modeled agricultural withdrawals as a function of the extent and efficiency of irrigation. We did not model livestock and other agricultural uses, which are typically a small fraction of agricultural withdrawals. Agriculture is unique among the three sectors because agricultural withdrawals depend strongly on climate (as evaporative demand) as well as socioeconomic drivers.

To estimate agricultural withdrawals and consumptive use (U_{ag} and C_{ag}), we first projected country-level irrigated area, then spatially distributed the irrigated area within

each country, and used climate projections to estimate the consumptive use over the projected irrigated area. We explicitly projected changes in spatial extent of irrigation in order to incorporate the effect of climate over irrigation areas.

4.1.1. Irrigated area projections by country

Country-level projections of irrigated area were performed using mixed effects regression¹² of *area equipped for irrigation* ($AEI_{i,t}$) from FAO (2013)¹³ for country at year as a function of the socioeconomic variables (see Table 1). To prevent projections from exceeding available agricultural land, the response variable was modeled as the logit-transformed proportion of agricultural land equipped for irrigation ($P_{i,t}$) for country i in year t , where $A_{ag,i}$ is the total agricultural area including both irrigated and rainfed agriculture for country i .

Table 1 | **Variables Used in Projection of Future Water Demand**

VARIABLE	ABBREVIATION	SOURCES
Area equipped for irrigation	AEI	FAO 2013 ^a
Agricultural land area	$A_{ag,i}$	FAO 2013 ^a
Irrigation efficiency	WRR	FAO 2013 ^a , Rohwer et al. 2007 ^b
Industrial water withdrawals	U_{ind}	FAO 2013 ^c
Domestic water withdrawals	U_{dom}	FAO 2013 ^c
Gross domestic product per capita	GDPPC	World Bank 2013 (GDP); ^d UN DESA 2013 (population) ^e
Urbanization	URBAN	UN DESA 2013 ^f
Baseline water stress	BWS	Gassert et al. 2013 ^g
Population density	POPDENS	UN DESA 2013 (population); ^e World Bank 2013 (land area) ^d
World population	PW	FAO 2013 ^c

a. Food and Agriculture Organization of the United Nations (FAO), "FAOSTAT," n.d., <http://faostat3.fao.org/home/index.html>.

b. Janine Rohwer, Dieter Gerten, and Wolfgang Lucht, *Development of Functional Types of Irrigation for Improved Global Crop Modelling* (Potsdam, 2007), <https://www.pik-potsdam.de/research/publications/pikreports/files/pr104.pdf>.

c. Food and Agriculture Organization of the United Nations (FAO), "AQUASTAT - FAO's Information System on Water and Agriculture," n.d., <http://www.fao.org/nr/water/aquastat/main/index.stm>.

d. World Bank, "World Development Indicators," 2013, <http://data.worldbank.org/data-catalog/world-development-indicators>.

e. United Nations Department of Economic and Social Affairs (UN DESA), "World Population Prospects: The 2012 Revision," 2013, http://esa.un.org/wpp/ASCII-Data/DISK_NAVIGATION_ASCII.htm.

f. United Nations Department of Economic and Social Affairs (UN DESA), "World Urbanization Prospects," 2012, <http://esa.un.org/unup/CD-ROM/Data-Sources.htm>.

g. Francis Gassert et al., *Aqueduct Global Maps 2.0*, Working Paper (Washington, DC: World Resources Institute, 2013), <http://www.wri.org/publication/aqueduct-metadata-global>.

Note: Baseline water stress (BWS) was spatially aggregated to the country scale using a weighting scheme specific to each sector. For industrial withdrawals, BWS was weighted using the Nighttime Lights;^h for domestic withdrawals using the Gridded Population of the World;ⁱ and for area irrigated using the Global Map of Irrigation Area.^j For all projections, BWS was held constant at the 2010 level.

h. NOAA National Geophysical Data Center and (NGDC), "Version 4 DMSP-OLS Nighttime Lights Time Series," 2010, <http://www.ngdc.noaa.gov/dmsp/downloadV4composites.html>.

i. Center for International Earth Science Information Network (CIESIN), Columbia University, United Nations Food and Agriculture Organization (FAO), and Centro Internacional de Agricultura Tropical (CAIT), "Gridded Population of the World Version 3 (GPWv3): Population Count Grid, Future Estimates," 2005, <http://sedac.ciesin.columbia.edu/gpw>.

j. Stefan Siebert et al., *Global Map of Irrigation Areas (GMIA) Version 5*, 2013, <http://www.fao.org/nr/water/aquastat/irrigationmap/index10.stm>.

$$P_{i,t} = \frac{AEI_{i,t}}{A_{ag,i}}$$

We fit coefficients (β) to predictor variables (X), including country-specific intercepts ($b_{o,i}$) to allow for idiosyncrasies among countries caused by specific policies, climate, or other unmodeled characteristics of countries, and world population (PW) to implicitly account for international agricultural trade.

$$\log\left(\frac{P_{i,t}}{1 - P_{i,t}}\right) = \beta_0 + \beta_{PW}PW + \beta_1 X_{1,i,t} + \beta_2 X_{2,i,t} + \dots + \beta_k X_{k,i,t} + b_{o,i} + b_{PW,i}PW + \epsilon_{i,t}$$

All predictor variables (X) were log transformed prior to fitting. We determined the final list of predictors (Table A3 in Appendix) by backward-stepwise regression using Akaike's Information Criterion (AIC).¹⁴ The model R^2 was 0.99, with the fixed effects (no country-specific effects) explaining 53 percent of the variation (see Table A3).

We converted projections obtained from the regression model to area actually irrigated ($A_{irr,i}$) by using the inverse-logit function to calculate predicted proportion $\hat{P}_{i,t}$, multiplying by $A_{ag,i}$, which was assumed to remain constant over the projection interval,¹⁵ and finally by multiplying by the ratio of *area actually irrigated* (AAI) to *area equipped for irrigation* (AEI) derived from the Global Map of Irrigation Area version 5 (GMIA v5),¹⁶ which was also assumed to remain constant:

$$A_{irr} = \hat{P}_{i,t} A_{ag,i} \frac{AAI_i}{AEI_i}$$

4.1.2. Spatial distribution of irrigated area

The country-level predictions were distributed spatially within countries to pixels based on the *likelihood of irrigation expansion* (LIE) dataset of Neumann et al. (2011).¹⁷ LIE assigns pixels into one of 10 classes ranging from 0 (zero likelihood) to 0.9 (highest likelihood) that were modeled from biophysical factors, such as humidity and slope, and socioeconomic and governance components such as corruption and GDP. For each country and scenario, we computed the projected change in irrigation

area ($\Delta A_{irr,i}$) as the difference between the projected area for the target year and the baseline year (2010):

$$\Delta A_{irr,i} = A_{irr,i,targetyear} - A_{irr,i,baselineyear}$$

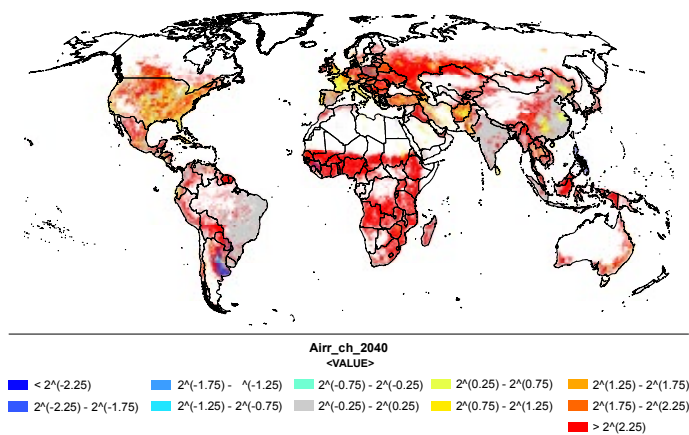
We then determined the area available for expansion (AAE) in each LIE class (l) and country (i) as the difference between AEI and AAI derived from GMIA v5:

$$AAE_{l,i} = AEI_{l,i} - AAI_{l,i}$$

In the original LIE dataset, cells with irrigation exceeding 10 percent of the cell area were classified as 0 percent likelihood to expand, but we reclassified those cell values to the highest class ($l = 0.9$) since in many of those areas, remaining agricultural land was equipped for irrigation though not currently irrigated. We also reclassified countries missing from the LIE dataset (see Appendix A) to the lowest likelihood class ($l = 0.3$) to allow extremely high levels of global excess to be distributed in these countries if needed.

We distributed positive values of $\Delta A_{irr,i}$ in three steps until either all land needed for expansion was distributed or all available land in a country was filled. First we distributed $\Delta A_{irr,i}$ to area equipped for irrigation but not currently irrigated ($AEI_l - AAI_l$) starting with the highest likelihood class until available land was filled, then proceeded to the next lower likelihood class. Second, we distributed any remaining $\Delta A_{irr,i}$ within areas unequipped for irrigation but likely to be irrigated in each country ($A_{ag,i} - AEI_l$), up to a doubling of irrigated area in each class above the first step. Finally, any $\Delta A_{irr,i}$ in excess of the available area in a country was distributed globally, proportionally to remaining available area by descending likelihood class, to essentially allow for agricultural trade between countries. For countries in which irrigated area was projected to decline, we distributed negative values of $\Delta A_{irr,i}$ in reverse order of probability (i.e., removed from least likely to be expanded). We generated one estimate of the extent of irrigated area for each of the target years 2020, 2030, and 2040.

Figure 3 | **Projected Change in Area Irrigated in 2040 as a Ratio of 2010 Values**



4.1.3. Irrigation consumptive use

Agricultural water use from irrigated area was estimated following the FAO methodology of Frenken and Gillet (2012)¹⁸ for *irrigation consumptive use (ICU)* excluding crop-specific evapotranspiration factors. *ICU* is the annual depth of water needed to fulfill the deficit between what crops could consume with ample water and what they would consume under rainfed conditions. We calculated *ICU* as *potential evapotranspiration* minus *actual evapotranspiration*:

$$ICU = PET - AET$$

We calculated monthly potential evapotranspiration (*PET*) using the Priestley-Taylor (1972)¹⁹ formulation following McMahon et al. (2013).²⁰ We computed reference *PET* ignoring crop-specific coefficients because of the difficulty of predicting future crop choice. We obtained actual evapotranspiration (*AET*) directly from GLDAS-2 and the CMIP5 models as latent heat flux converted to water volume using the latent heat of vaporization (*Latent Heat Flux* in GLDAS-2²¹ and *hfls* in CMIP5).²²

Finally, we bias-corrected the GCM-derived annual estimates of *ICU* to GLDAS-2 using quantile-quantile matching as described in section 2.2. We assumed that all irrigated land is irrigated at the rate needed to fulfill *ICU* such that *total agricultural consumptive use* (C_{ag}) is equal to $ICU \times A_{irr}$.

4.1.4 Irrigation water withdrawals

Agricultural withdrawals were calculated using FAO methodology²³ for *irrigation water withdrawals (IWW)* accounting for additional nonconsumptive water use by paddy lands²⁴ and potential improvements in irrigation efficiency. We derived *IWW*, or agricultural water withdrawals (U_{ag} , Figures A3 and A4 in Appendix), from *irrigation water requirement (IWR)* and irrigation efficiency (*WRR*):

$$U_{ag} = IWW = \frac{IWR}{WRR}$$

Irrigation water requirement (IWR) is a measure of the water required for optimal crop growth including consumptive and nonconsumptive purposes. We computed *IWR* from irrigation consumptive use, adjusting for paddy land:

$$\begin{aligned} IWR &= ICU \times A_{irr} + 0.2 \times A_{rice} \\ &= C_{ag} + 0.2 \times A_{rice} \end{aligned}$$

where A_{irr} and A_{rice} are area actually irrigated and area under paddy irrigation (rice in MIRCA 2000v1.1),²⁵ respectively; and 0.2 represents additional nonconsumptive water use from the depth of rice paddy irrigation in meters, which is returned to the surface waters following harvest.²⁶ Excess evaporation of surface water in rice paddy over the growing season is ignored by the FAO methodology.

The *water requirement ratio (WRR)*, also referred to as irrigation efficiency, is the amount of water required by crops to meet their evapotranspiration needs, divided by the amount of water actually withdrawn to meet those needs.²⁷ This ratio is less than 1 because of water leakage or other losses in the irrigation system on the way from the source to the plant.

We projected improvements in *WRR* using a cross-sectional country-scale regression based on the relationships between the average *WRR* and historical estimates of the same SSP driver variables used for projecting $A_{irr,i}$ (see section 4.1.1). We obtained historic values for *WRR* from FAO AQUASTAT (2013)²⁸ and Rohwer et al. (2007).²⁹ These sources use complementary methodologies so the

two values for each country were averaged. Time series data were not available for these variables; AQUASTAT estimates were from various years with a mean of 2003 (range of 1987 to 2012) and Rohwer et al. estimates were from 1997–2005 (actual year not specified). Terms in the regression were selected using backward stepwise selection via AIC. The resulting model contained only GDP per capita (coefficient = -0.39 ± 0.13 , $P < 0.001$, $R^2 = 0.355$).

4.2. Domestic and Industrial Withdrawals

Future projections of industrial and domestic water withdrawals were developed using an approach similar to that used for irrigated area (see section 4.1.1). Mixed-effects regression models were developed for country-level withdrawals as a function of socioeconomic drivers (see Table 1); the coefficients derived from these regressions were then applied to SSP projections³⁰ of the socioeconomic drivers to determine future country level water use.

The model for the industrial withdrawals included country-specific time effects ($b_{YEAR,i}$) as well as country-specific intercepts ($b_{o,i}$):

$$U_{ind,i,t} = \beta_0 + \beta_{YEAR} YEAR + \beta_1 X_{1,i,t} + \beta_2 X_{2,i,t} + \beta_k X_{k,i,t} + b_{o,i} + b_{YEAR,i} YEAR + \epsilon_{i,t}$$

where $U_{ind,i,t}$ is industrial water withdrawals for country i and time t , β_k represents the intercept and coefficients for variable k , b represents country-specific coefficients, and $\epsilon_{i,t}$ is the residual variation distributed as $N(0, 1)$ (Table A4 in Appendix).

The $b_{o,i}$ and $b_{YEAR,i}$ terms were required to produce adequate fits to the data, though projections became sensitive to short-term trends in the observed withdrawal data. If a country displayed a large increase (or decrease) in withdrawals over the observed time frame, the model would project a similarly large increase (or decrease) over time, resulting in extreme and unrealistic future projections. To reduce this effect we Winsorized³¹ 20 percent of the $b_{YEAR,i}$ terms as follows:

$$b_{YEAR,i} = \begin{cases} b_{YEAR,80} & \text{if } b_{YEAR,i} \geq b_{YEAR,80} \\ b_{YEAR,i} & \text{if } |b_{YEAR,i}| > b_{YEAR,80} \\ -b_{YEAR,80} & \text{if } b_{YEAR,i} \leq -b_{YEAR,80} \end{cases}$$

where $b_{YEAR,80}$ is the 80th percentile value of the distribution of the $|b_{YEAR,i}|$.

In addition, we assigned countries with positive slopes and fewer than three time points of observed data the global average time effect (i.e., $b_{YEAR,i}$ set to 0). This results in relatively conservative estimates of the rate of increase in industrial withdrawals.

The projections were sensitive to covariates included in the regression model, particularly quadratic and higher power terms and interactions. Therefore, we applied several procedures to limit overfitting: (1) Limited model complexity: interactions were limited to two-way between linear terms only, and terms were assumed to be linear except GDP per capita and population density, which were allowed to be quadratic; and (2) generated models with both AIC and Bayes' Information Criterion (BIC) as the goodness-of-fit measure for step-down regression.³² BIC penalizes additional predictor variables more heavily and thus is more conservative than AIC. Projected country-level withdrawals were a simple average of the values from the AIC and the BIC selected models.

The model for domestic withdrawals (Table A5 in Appendix) was the same except that it did not include country-specific time effects.

4.2.1. Spatial disaggregation

We spatially disaggregated industrial and domestic projected withdrawals from countries (i) to pixels (p) using 0.5° projections by Special Report on Emissions Scenarios (SRES) scenario from IIASA (2009):³³

$$U_{ind,p} = U_{ind,i} \frac{GDP_p}{\sum_{p \in i} GDP_p}$$

SRES scenarios were matched with SSPs as suggested by van Vuuren and Carter (2013): A2 and B2 for SSP3 and SSP2, respectively since spatial projections based on SSPs were not yet available.³⁴ Industrial and domestic withdrawals were disaggregated using identical methodologies except industrial withdrawals used future projections of GDP while domestic withdrawals used projections of population (Figures A5 and A7 in Appendix).

4.2.2. Consumptive use

Industrial and domestic consumptive use (C_{ind} and C_{dom}) were calculated for all target years by multiplying withdrawals by the 2025 projection of industrial and domestic consumptive use ratios (consumptive use / withdrawals), respectively, from Shiklomanov and Rodda.³⁵

Total withdrawals and total consumptive use (U_t and C_t) were equal to the sum of withdrawals and consumptive use for each of the three sectors, respectively.

5. INDICATORS

From these data, we generated four global indicators—change in water demand (withdrawal), change in water supply, change in water stress, and change in intra-annual (seasonal) variability—for three future periods centered around 2020, 2030, and 2040, and three combinations of climate and socioeconomic scenarios: RCP 4.5/SSP2, RCP8.5/SSP2, and RCP8.5/SSP3 (selection of RCP and SSP scenarios is described in Appendix). RCP 4.5/SSP2 is cautiously optimistic climate scenario with a business-as-usual socioeconomic scenario; RCP8.5/SSP2 is business-as-usual for both scenarios; RCP8.5/SSP3 is the business as usual climate scenario with a pessimistic socioeconomic scenario. Each indicator was calculated relative to a historical (baseline) period of 1950–2010, selected to match Gassert et al.³⁶ Results were computed separately for each GCM ensemble then summarized as the weighted mean of the members (\bar{x}) such that each of the six GCMs (n) was weighted equally regardless of the number of members (m):

$$\bar{x} = \frac{1}{n} \sum_i^n \left(\frac{1}{m_i} \sum_j^{m_i} x_{i,j} \right)$$

We also computed a weighted coefficient of variance between ensemble members as a measure of model agreement:

$$cv = \frac{1}{\bar{x}} \sqrt{\frac{\sum 1/m_i (x_{i,j} - \bar{x})^2}{\sum 1/m_i}}$$

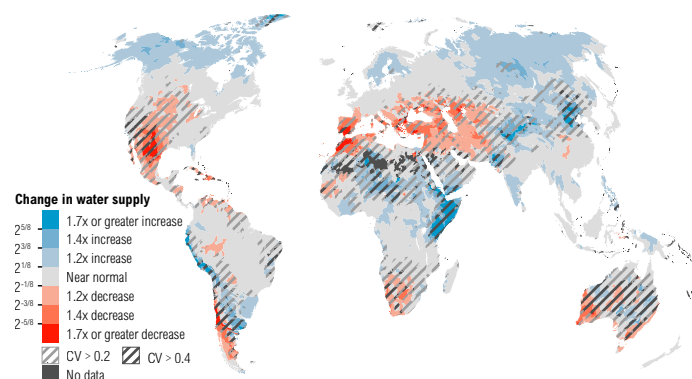
All indicators are computed and displayed at the catchment scale.

5.1. Water Supply

Total blue water (renewable surface water) was our indicator of water supply. Projected change in total blue water is equal to the 21-year mean around the target year divided by the baseline period of 1950–2010.

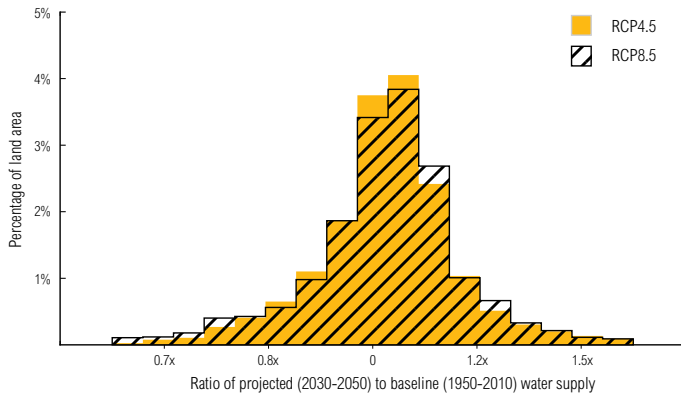
Results show drying in the midlatitudes, likely because of the anticipated poleward Hadley cell expansion caused by increasing global temperatures (see Figure 4).³⁷ There is considerable variability between GCM projections for future water supply, especially in areas where mean projected changes are high and around the boundaries between areas becoming wetter and areas becoming drier. Results between scenarios show similar spatial patterns, with slightly greater magnitude of change under high emissions scenario RCP8.5 (see Figure 5). Climate factors in cautiously optimistic scenario RCP4.5 begin to deviate from RCP8.5 only in 2020 (Figure A1 in Appendix), so only small differences between the scenarios are expected.

Figure 4 | **Weighted Mean Projected Change in Water Supply from Baseline (1950–2010) to Future Period (2030–50) under Business-as-Usual Scenario RCP8.5/SSP2**



Hashing shows the weighted coefficient of variance between model members, a measure of model agreement. No hashing, light hashing, and dark hashing correspond to standard deviations equivalent to 0–1, 1–2, and >2 categories on the legend, respectively.

Figure 5 | Histograms of Land Area by Projected Change in Water Supply from Baseline (1950–2010) to Future Period (2030–50) under Scenarios RCP4.5 and RCP8.5



Note: X-axis is on a log scale.

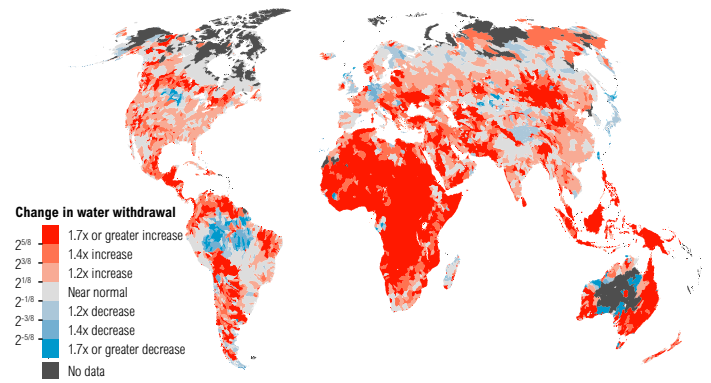
5.2. Water Demand

Water demand was measured as water withdrawals. Projected change in water withdrawals is equal to the summarized withdrawals for the target year, divided by the baseline year, 2010. Since irrigation consumptive use varies based on climate, we generated unique estimates of U_{ag} and C_{ag} for each year. Estimates for U_{ag} and C_{ag} for each ensemble member, scenario, and target year are the mean of the 21-year window around the target year.

Projections show substantial relative increases in water demand in developing nations, particularly in central Africa and other undeveloped areas where baseline water demand is very low (see Figure 6). This reflects assumptions in the SSPs of rapid urbanization and population growth in developing countries. While relative water demand growth is projected to be high, many of the least developed areas are starting from very low levels of water use, and remain at low stress levels through the coming decades.

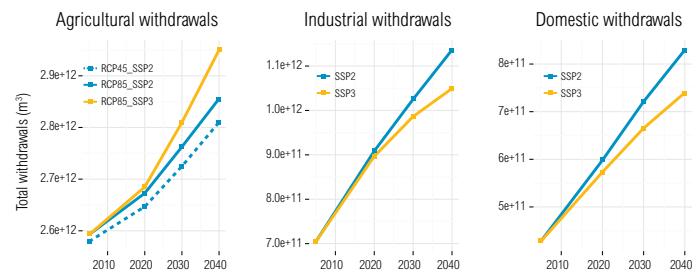
Additionally, projections show higher industrial and domestic demand under the more economically positive scenario (SSP2), presumably because of increasing affluence and energy demand, and more agricultural demand under the pessimistic (SSP3) scenario, because of higher population (Figure 7). Areas with decreasing water demand primarily reflect expected urbanization patterns around the world.

Figure 6 | Projected Change in Water Demand from Baseline (2010) to Future Period (2030–50) under Business-as-usual scenario RCP8.5/SSP2



Note: This map is on the same scale as that in Figure 4 to show the more rapid change in demand over supply.

Figure 7 | Global Projected Water Withdrawals by Sector and Scenario



5.3. Water Stress

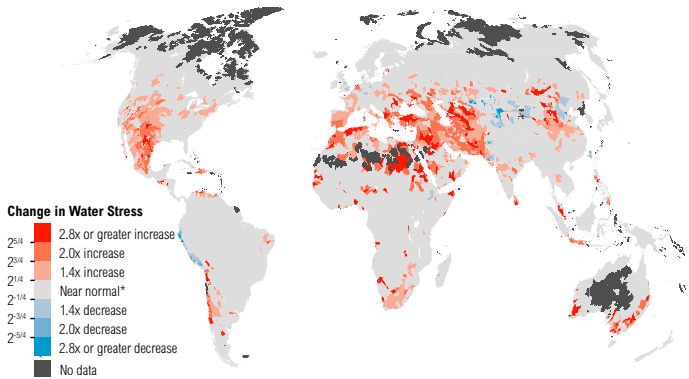
Water stress (WS) is an indicator of competition for water resources and is defined informally as the ratio of demand for water by human society divided by available water. It is also commonly known as the withdrawals-to-availability ratio³⁸ or relative water demand.³⁹ Following Gassert et al., we computed water stress as the ratio of water withdrawals to available blue water on an average annual basis:

$$WS_t = \frac{Ut_t}{Ba_{[t-10:t+10]}}$$

Available blue water (Ba) is flow-accumulated runoff minus upstream consumptive use computed over hydrological catchments.⁴⁰ We computed projected available blue water as the mean of the 21-year period around the

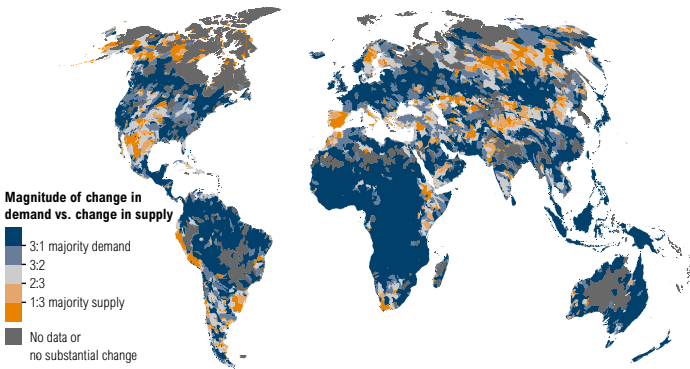
target year using runoff from each year with the mean consumptive use for the target year. Change estimates use the 1950–2010 baseline period for available blue water. Results show rapid increases in stress across much of the Mediterranean, Central Asia, and the southwest of North America (Figure 8). Stress changes are driven primarily by increases in water demand (Figure 9); however, exceptional increases in stress from diminishing water supply along the midlatitudes in the southwest of North America and the Mediterranean are also evident. Large portions of Africa are also projected to have rapid relative increases in demand, but remain at low stress levels.

Figure 8 | **Projected Change in Water Stress from Baseline (1950–2010) to Future Period (2030–50) under Scenario RCP8.5/SSP2**



*Regions that increase in stress but remain at low stress levels (<0.1) and regions that decrease in stress but remain at extremely high stress levels (>0.8) are shown as “near normal.”

Figure 9 | **Relative Contribution of Changes in Water Demand vs. Water Supply to Projected Change in Water Stress from Baseline (1950–2010) to Future Period (2030–50) under Scenario RCP8.5/SSP2**



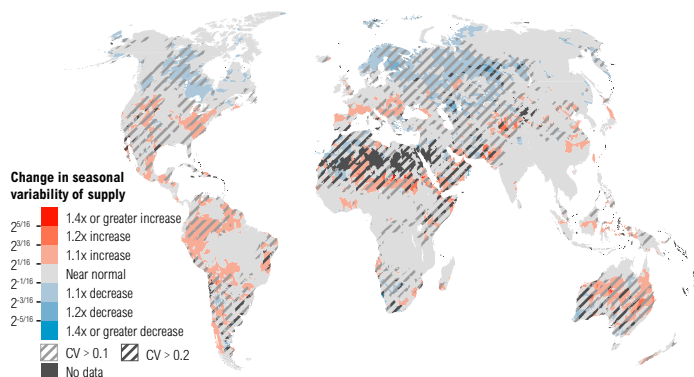
Note: Change in water stress in orange areas is primarily driven by climate effects on water supply.

5.4. Seasonal Variability

Seasonal variability (SV) is an indicator of the variability between months of the year. Increasing SV may indicate wetter wet months and drier dry months, and higher likelihood of droughts or wet periods. We used the within-year coefficient of variance between monthly total blue water as our indicator of seasonal variability of water supply. We calculated the coefficient of variance between months for each year, then estimated projected change in seasonal variability as the 21-year mean around the target year over the baseline period mean.

The signal for changes in seasonal variability is notably weak with substantial changes not appearing until the end of the projection period (Figure 10).

Figure 10 | **Projected Change in Seasonal Variability from Baseline (1950–2010) to Future Period (2030–50) under Scenario RCP8.5/SSP2**



Note: Hashing shows the weighted coefficient of variance between model members, a measure of model agreement. No hashing, light hashing, and dark hashing correspond to standard deviations equivalent to 0–1, 1–2, and >2 categories on the legend, respectively.

6. DISCUSSION

Projections show substantial increases in water stress across many regions including the Mediterranean, the Middle East, the North American West, eastern Australia, western Asia, northern China, and Chile, within a relatively short span of time.

The relative dominance of changes in demand over changes in supply raises several points of emphasis. First, growth in demand is as important as—if not more important than—changes in supply. This is of significant concern given poor model performance and poorly quantified uncertainty in water demand projections.⁴¹

Second, water managers have an opportunity to intervene in water resource availability by curtailing increases in demand. Our projections assume that water demand will follow a trajectory similar to that of the past decade. This is a weak assumption, and shows only one set of possible future outcomes. Globally, actors' ability to increase investment in efficiency and conservation as well as to pursue more conservative water allocation schemes could dramatically affect future stress levels.

Third, though changes in water demand outweigh changes in water supply, the areas in which water supply is projected to decrease may be especially sensitive. The regions with the highest rates of drying—the North American Southwest, wide swaths of the Mediterranean, South Africa, Australia's Murray-Darling basin, and the Russian grain belt—are already under high water stress and include several of the world's major agricultural areas. Adapting to decreasing water supply in regions where water is already fully allocated will be a significant challenge. These changes in water supply can be mitigated in part by rapid reduction in global carbon emissions. The low emissions (RCP4.5) scenario shows slower rates of change relative to the high emissions (RCP8.5) scenario, demonstrating the benefit of aggressive carbon emissions reductions within the next few decades.

Finally, even areas that are not expected to get drier may be exposed to increased seasonal variability of water supply. This may be indicative of higher probability of drought and wet periods. Variability, compounded with the uncertainty in future changes, means that decision-makers must plan for a wide range of possible outcomes. Both a 30 percent increase in surface water supply and a 30 percent decrease within the next three decades are not out of the realm of possibility in areas such as southern California.

ENDNOTES

- Charles J. Vörösmarty, Claudia Pahl-Wostl, and Anik Bhaduri, "Water in the Anthropocene: New Perspectives for Global Sustainability," *Current Opinion in Environmental Sustainability* 5, no. 6 (December 2013): 535–38, doi:10.1016/j.cosust.2013.11.011.
- See, among others, Simon N. Gosling and Nigel W. Arnell, "A Global Assessment of the Impact of Climate Change on Water Scarcity," *Climatic Change*, 2013, 1–15, doi:10.1007/s10584-013-0853-x; N. Hanasaki et al., "A Global Water Scarcity Assessment under Shared Socio-Economic Pathways – Part 2: Water Availability and Scarcity," *Hydrology and Earth System Sciences* 17 (2013): 2393–2413, doi:10.5194/hess-17-2393-2013; Michelle T. H. van Vliet et al., "Global River Discharge and Water Temperature under Climate Change," *Global Environmental Change* 23, no. 2 (April 2013): 450–64, doi:http://dx.doi.org/10.1016/j.gloenvcha.2012.11.002; Jacob Schewe et al., "Multimodel Assessment of Water Scarcity under Climate Change," *Proceedings of the National Academy of Sciences*, December 16, 2013, doi:10.1073/pnas.1222460110; S. Hagemann et al., "Climate Change Impact on Available Water Resources Obtained Using Multiple Global Climate and Hydrology Models," *Earth System Dynamics* 4 (2013): 129–44, doi:10.5194/esd-4-129-2013.
- Karl E. Taylor, Ronald J. Stouffer, and Gerald a. Meehl, "An Overview of CMIP5 and the Experiment Design," *Bulletin of the American Meteorological Society* 93, no. 4 (April 2012): 485–98, doi:10.1175/BAMS-D-11-00094.1.
- International Institute for Applied Systems Analysis (IIASA), "Shared Socioeconomic Pathways (SSP) Database (version 0.93)," <https://secure.iiasa.ac.at/web-apps/ene/SspDb>.
- Taylor, Stouffer, and Meehl, "An Overview of CMIP5 and the Experiment Design."
- Simon J. Mason, "From Dynamical Model Predictions to Seasonal Climate Forecasts," in *Seasonal Climate: Forecasting and Managing Risk*, ed. Alberto Troccoli et al. (Boston: Springer Verlag, 2007), 209–40.
- M. Rodell et al., "The Global Land Data Assimilation System," *Bulletin of the American Meteorological Society* 85, no. 3 (2004): 381–94, <http://dx.doi.org/10.1175/BAMS-85-3-381>. Available online at <http://disc.sci.gsfc.nasa.gov/hydrology/data-holdings>. GLDAS-2 was used for bias correction to provide continuity with Gassert et al., *Aqueduct Global Maps 2.1: Constructing Decision-Relevant Global Water Risk Indicators*. GLDAS-2 was selected based on evaluation of alternatives that examined correlation with runoff fields that are based on *in-situ* gauge data by B. M. Fekete, C. J. Vörösmarty, and W. Grabs, "High-Resolution Fields of Global Runoff Combining Observed River Discharge and Simulated Water Balances," *Global Biogeochemical Cycles* 16, no. 3 (2002): 10–15, doi:10.1029/1999GB001254.
- Stewart Coles, *An Introduction to Statistical Modeling of Extreme Values* (London: Springer-Verlag, 2001), <http://www.springer.com/statistics/statistical+theory+and+methods/book/978-1-85233-459-8.col>.
- Gassert et al., *Aqueduct Global Maps 2.1: Constructing Decision-Relevant Global Water Risk Indicators*.
- The primary differentiating factor between domestic (i.e., urban) and industrial or agricultural withdrawals is that domestic withdrawals are supplied by a public distribution system while the others are not. Agricultural withdrawals are the amount of water used above and beyond rainfed agriculture. See: A. Kohli, K. Frenken, and C. Spottorno, *Disambiguation of Water Statistics*, May 2012.
- Brian C O'Neill et al., "Meeting Report of the Workshop on The Nature and Use of New Socioeconomic Pathways for Climate Change Research, Boulder CO, November 2–4, 2011," 2012, 1–37, <http://www.isp.ucar.edu/socio-economic-pathways>; O'Neill et al., "A New Scenario Framework for Climate Change Research: The Concept of Shared Socioeconomic Pathways," *Climatic Change*, 112, no. 3 (2014): 387–400.
- Judith D. Singer and John B. Willett, *Applied Longitudinal Data Analysis* (New York: Oxford University Press, 2003); Jose C. Pinheiro and Douglas M. Bates, *Mixed-Effects Models in S and S-Plus* (New York: Springer Verlag, 2000).
- Food and Agriculture Organization of the United Nations (FAO), "FAO-STAT," (database).
- H Akaike, "A New Look at the Statistical Model Identification," *IEEE Transactions on Automatic Control* 19, no. 6 (1974): 716–23, doi:10.1109/TAC.1974.1100705.
- We did not attempt to model change in total agricultural land area, though agricultural land area has not increased rapidly in the recent past. Global agricultural land area increased 12% from 1960 to 2011, and the most recent 15 years from a peak in 1994 to the highest point in 2011 was only a 1% increase. Author's calculations based on Food and Agriculture Organization of the United Nations (FAO), "FAOSTAT."
- Siebert et al., *Global Map of Irrigation Areas (GMA) Version 5*.
- Kathleen Neumann et al., "Exploring Global Irrigation Patterns: A Multi-level Modelling Approach," *Agricultural Systems* 104, no. 9 (November 2011): 703–13, doi:http://dx.doi.org/10.1016/j.agry.2011.08.004. areas that are equipped for irrigation have almost doubled in size over the past 50 years and further expansions are expected for the future, to meet a growing food demand. For developing countries, the Food and Agriculture Organization of the United Nations (FAO)
- Karen Frenken and Virginie Gillet, *Irrigation Water Requirement and Water Withdrawal by Country*, 2012, http://www.fao.org/nr/water/aquastat/water_use_agr/index4.stm.
- C. H. B. Priestley and R. J. Taylor, "On the Assessment of Surface Heat Flux and Evaporation Using Large-Scale Parameters," *Monthly Weather Review* 100, no. 2 (February 1, 1972): 81–92, doi:10.1175/1520-0493(1972)100<0081:OTAOSH>2.3.CO;2.
- T. a. McMahon et al., "Estimating Actual, Potential, Reference Crop and Pan Evaporation Using Standard Meteorological Data: A Pragmatic Synthesis," *Hydrology and Earth System Sciences* 17, no. 4 (April 10, 2013): 1331–63, doi:10.5194/hess-17-1331-2013.
- Hualan Rui and Hiroko Beaudoin, *README Document for Global Land Data Assimilation System Version 2 (GLDAS-2) Products (Vol. 2)*, 2013.
- World Climate Research Programme Coupled Model Intercomparison Project, "CMIP5 – Data Description List of Requested Model Output," 2013.
- Frenken and Gillet, *Irrigation Water Requirement and Water Withdrawal by Country*.
- Felix T. Portmann, Stefan Siebert, and Petra Döll, "MIRCA2000—Global Monthly Irrigated and Rainfed Crop Areas around the Year 2000: A New High-Resolution Data Set for Agricultural and Hydrological Modeling," *Global Biogeochemical Cycles* 24, no. 1 (March 1, 2010): GB1011, doi:10.1029/2008GB003435.
- Ibid.

26. Frenken and Gillet, *Irrigation Water Requirement and Water Withdrawal by Country*.
27. Janine Rohwer, Dieter Gerten, and Wolfgang Lucht, *Development of Functional Types of Irrigation for Improved Global Crop Modelling* (Potsdam, 2007), <https://www.pik-potsdam.de/research/publications/pikreports/files/pr104.pdf>
28. Food and Agriculture Organization of the United Nations (FAO), "AQUA-STAT - FAO's Information System on Water and Agriculture."
29. Rohwer, Gerten, and Lucht, *Development of Functional Types of Irrigation for Improved Global Crop Modelling*.
30. International Institute for Applied Systems Analysis (IIASA), "Shared Socioeconomic Pathways (SSP) Database (version 0.93)."
31. Cecil Hastings Jr. et al., "Low Moments for Small Samples: A Comparative Study of Order Statistics," *The Annals of Mathematical Statistics* 18, no. 3 (1947): 413–26, <http://www.jstor.org/stable/2235737>.
32. G. E. Schwarz, "Estimating the Dimension of a Model," *Annals of Statistics* 6, no. 2 (1978): 461–64, doi:10.1214/aos/1176344136.
33. International Institute for Applied Systems Analysis (IIASA), "Greenhouse Gas Initiative (GGI) Scenario Database Ver. 2.0," 2009, <http://www.iiasa.ac.at/Research/GGI/DB/>.
34. Detlef P. van Vuuren et al., "The Use of Scenarios as the Basis for Combined Assessment of Climate Change Mitigation and Adaptation," *Global Environmental Change* 21, no. 2 (May 2011): 575–91, doi:10.1016/j.gloenvcha.2010.11.003.
35. I. A. Shiklomanov and John C. Rodda, eds., *World Water Resources at the Beginning of the Twenty-First Century*, International Hydrology Series (Cambridge University Press, 2004).
36. Gassert et al., *Aqueduct Global Maps 2.1: Constructing Decision-Relevant Global Water Risk Indicators*.
37. Sarah M. Kang and Jian Lu, "Expansion of the Hadley Cell under Global Warming: Winter versus Summer," *Journal of Climate* 25, no. 24 (September 21, 2012): 8387–8393, doi:10.1175/JCLI-D-12-00323.1.
38. Joseph Alcamo et al., "Global Estimates of Water Withdrawals and Availability under Current and Future 'Business-as-Usual' Conditions," *Hydrological Sciences Journal* 48, no. 3 (June 1, 2003): 339–48, doi:10.1623/hysj.48.3.339.45278.
39. Charles J. Vörösmarty et al., "Global Water Resources: Vulnerability from Climate Change and Population Growth," *Science* 289, no. 5477 (2000): 284–88, <http://www.sciencemag.org/cgi/doi/10.1126/science.289.5477.284>.
40. Gassert et al., *Aqueduct Global Maps 2.1: Constructing Decision-Relevant Global Water Risk Indicators*.
41. M. Flörke, S. Eisner, N. Hanasaki, Y. Masaki, Y. Wada, and M. Bierkens, "A Multi-Model Ensemble for Identifying Future Water-Scarcity Hotspots," in "Impacts World 2013: International Conference on Climate Change Effects," May 27–30, 2013, Potsdam, Germany. pp1–8. Available at http://www.climate-impacts-2013.org/files/hcaw_florke.pdf.

APPENDIX

A.1 Scenario selection

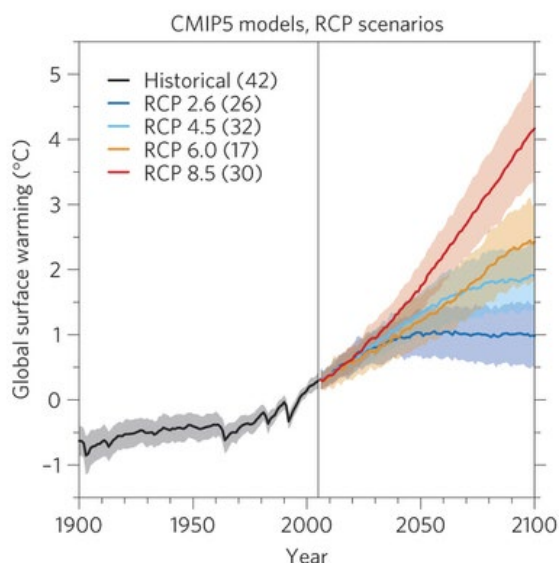
Water stress projections were based on a combination of future scenarios given by Representative Concentration Pathways (RCPs) and Shared Socioeconomic Pathways (SSPs).¹

RCPs specify the trajectory of radiative forcing (in W/m² with the endpoint value given in 2100) and thus drive the change in climate (Figure A1) and water availability simulated by Coupled Model Intercomparison Project Phase 5 (CMIP5) climate models. RCPs affected the projected water supply (calculated from runoff) and irrigation water demand. We chose two scenarios, a “business-as-usual” scenario of relatively unconstrained emissions and a “cautiously optimistic” scenario of stabilizing emissions. The business-as-usual scenario was RCP8.5, with CO₂ concentrations reaching ~1370 ppm by 2100 and global mean temperatures increasing by 2.6–4.8°C relative to 1986–2005 levels.² Current emissions track slightly above

emissions in this scenario.³ RCP4.5 represents the cautiously optimistic scenario, with emissions constrained to stabilize at ~650 ppm CO₂ and temperatures to 1.1–2.6°C by 2100. An additional benefit of these scenarios is that because they comprise the CMIP5 core experiments they have a greater number of models and ensemble members for download.⁴

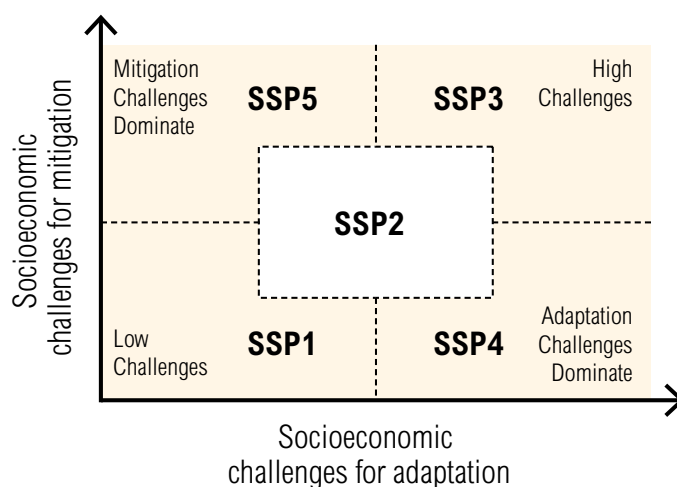
We used SSPs to define the primary socioeconomic drivers of water use. SSPs are defined along two axes (Figure A2):⁵ challenges for adapting to climate change, and challenges for mitigating climate change (i.e., reducing emissions). We chose two scenarios to represent a “business-as-usual” scenario, SSP2, and a “pessimistic” scenario, SSP3.⁶ The SSPs are defined in terms of three key variables: population, GDP, and urbanization, defined as the fraction of the population living in urban centers. SSP3 differs from SSP2 in having higher population growth, lower GDP growth, and a lower rate of urbanization, all of which potentially affect water usage (Figure A3).⁷ All SSP variables are provided at the national scale in five-year increments from 2005–2100.⁸

Figure A1 | **Projected Trends in Average Global Temperature Relative to 1986-2005 According to Scenarios Defined by the Representative Concentration Pathways**



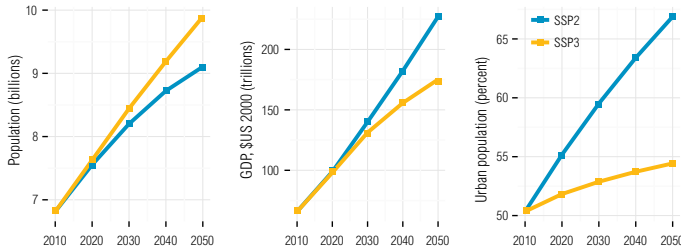
Source: Reto Knutti and Jan Sedláček, “Robustness and Uncertainties in the New CMIP5 Climate Model Projections,” *Nature Climate Change*, no. October (October 28, 2012): 1–5, doi:10.1038/nclimate1716.

Figure A2 | **Shared Socioeconomic Pathways in “Challenges Space”: Difficulty to Adapt to Climate Change (x-axis) and to Reduce Emissions and Prevent Climate Change (y-axis)**



Source: O'Neill et al., “A New Scenario Framework for Climate Change Research.”

Figure A3 | **Projected Trends in Three Drivers of SSP Scenarios: Population, GDP, and Fraction of Population Living In Urban Areas**



Source: International Institute for Applied Systems Analysis (IIASA), "Shared Socioeconomic Pathways (SSP) Database (version 0.93)," 2013, <https://secure.iiasa.ac.at/web-apps/ene/SspDb>.

A.2 Climate model selection

All projected climate data were obtained from general circulation models (GCMs) in the CMIP5 project, downloaded from the Program for Climate Model Diagnosis and Interpretation (PCMDI) CMIP5 portal.⁹ We selected six GCMs: CCSM4, CNRM-CM5, GFDL-ESM2M, INMCM4, MPI-ESM-LR, and MRI-CGCM3. These models were selected based on several criteria: a broad lineage of models from geographically and methodologically diverse modeling centers, the availability of required data for both RCP45 and RCP85, and, most importantly, their ability to reproduce the mean and standard deviation of historical runoff.

Specifically, Alkama et al. (2013)¹⁰ provided simulated runoff data for 15 CMIP5 models and observed runoff data from Dai et al. (2009).¹¹ For each CMIP5 model (*m*) and each of 18 major river basins (*b*), we calculated the proportion error (*E*) between the simulated and observed (*o*) mean or standard deviation of runoff:

$$E_{m,b} = \frac{X_{m,b} - X_{o,b}}{x_{o,b}}$$

where *x* is either the mean runoff or the standard deviation for the time period 1950–92. Within each basin, the $E_{m,b}$ for each of the 15 models were ranked in terms of the mean and standard deviation. The final six models were then chosen based on the averaged ranks (*K*) over all *n*=18 basins:

$$K = \frac{\sum_b^n K_{mean,b} + K_{sd,b}}{2n}$$

We used all of the available ensemble members for each model (Table A1), resulting in a total of 13 ensemble members for RCP4.5 and 17 members for RCP8.5. In addition to CMIP5 projection models, we also used observed climate data from 1950–2005 from the Global Land Data Assimilation System version 2.0 (GLDAS-2)¹² as a reference dataset to correct for bias in the CMIP5 model data.

Table A1 | **CMIP5 Models Used for Climate Data**

MODEL	INSTITUTION	RESOLUTION (DEGREES)	RCP4.5 MEMBERS	RCP8.5 MEMBERS
CCSM4	National Center for Atmospheric Research (U.S.)	1.25 × 0.9375	6	6
CNRM-CM5	National Center for Meteorological Research—European Center for Research and Advanced Training in Scientific Computation (France)	1.4 × 1.4	1	5
GFDL-ESM2M	NOAA Geophysical Fluid Dynamics Laboratory (U.S.)	2.5 × 2	1	1
INM-CM4	Institute for Numerical Mathematics (Russia)	2 × 1.5	1	1
MPI-ESM-LR	Max Planck Institute for Meteorology (Germany)	1.875 × 1.875	3	3
MRI-CGCM3	Meteorological Research Institute (Japan)	1.125 × 2.25	1	1

We downloaded several variables from each model to estimate monthly water runoff and agricultural irrigation demand (Table A2). Whereas total runoff was provided directly by the climate models, irrigation demand was calculated from potential and actual evapotranspiration (*PET* and *AET* respectively), themselves calculated from the variables listed in Table A2 (see below for details on this calculation). All climate data were downloaded as monthly totals or means and downscaled to 1°×1° using “conserve” resampling in the National Center for Atmospheric

Research (NCAR) Command Language.¹³ To ensure that data fully extended to the coastlines, missing values along the margins of landmasses were filled using the “FillNo-Data” function in the Geospatial Data Abstraction Library (GDAL),¹⁴ with smoothing iterations set to 1.

Table A2 | **Variables Obtained from GLDAS-2 and CMIP5 Climate Models**

VARIABLE	CMIP5 SHORT NAME	GLDAS-2 VARIABLE NAME
Surface runoff	—	Surface Runoff
Subsurface runoff	—	Subsurface Runoff
Total runoff	mrro	—
Air temperature at 2 m	tas	Near surface air temperature
Surface pressure	ps	Surface pressure
Surface downwelling shortwave radiation	rsds	Surface incident shortwave radiation
Surface net longwave radiation	—	Net Longwave Radiation
Surface downwelling longwave radiation	rlds	—
Surface upwelling longwave radiation	rlus	—
Latent heat flux	hfls	Latent heat flux

Note: See text for description of the regression models used. See Table 1 for explanation of abbreviations.

A.3 Agricultural water withdrawals

Table A3 | **Coefficients for Projection of Area Equipped for Irrigation**

VARIABLE	VALUE	STD.ERROR	P-VALUE
Intercept	15	4.17	0.00028
World Population (PW)	0.0009	0.00024	0.00044
POPSENS	1	2.40	0.54
POPSENS ²	0.7	0.78	0.35
GDPPC	-6	1.08	6.24E-09
GDPPC ²	0.52	0.078	2.18E-11
BWS	6	1.61	0.0002
BWS ²	-0.22	0.091	0.015
PW × GDPPC	-0.00011	3.56E-05	0.0018
POPSENS × GDPPC	-0.6	0.35	0.10
POPSENS × BWS	-0.7	0.24	0.003
GDPPC × BWS	-1.8	0.47	0.0002
POPSENS ² × GDPPC	-0.3	0.11	0.009
POPSENS ² × BWS	-0.34	0.080	1.92E-05
GDPPC ² × BWS	0.14	0.036	9.44E-05

Note: See text for description of the regression models used. See Table 1 for explanation of abbreviations.

Figure A4 | **Agricultural Water Withdrawals, 2010**
(m³ per 5 arc-minute cell)

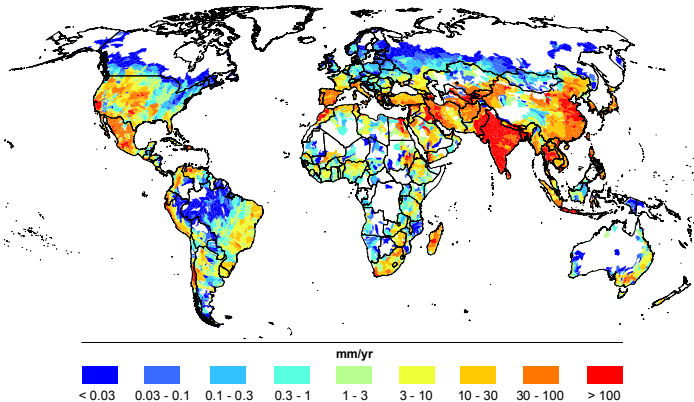
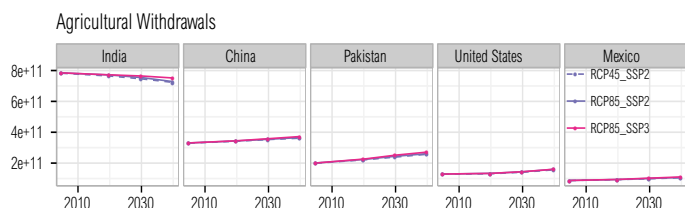


Figure A5 | **Projected Agricultural Withdrawals for the Top Five Agricultural Water Users, 2010**
(square meters)



A.4 Industrial and domestic water withdrawals

Table A4 | **Regression Coefficients for Projecting Future Industrial Withdrawals**

VARIABLE	VALUE	STD.ERROR	P-VALUE
AIC model			
Intercept	3	1.63	0.045
GDPPC	-1.6	0.99	0.11
URBAN	0.06	0.018	0.0013
BWS	0.4	0.11	9.73E-05
GDPPC ²	0.3	0.16	0.094
GDPPC × URBAN	-0.015	0.0047	0.0010
URBAN × BWS	-0.007	0.0018	0.00020
BIC model			
Intercept	0.8	0.73	0.27
GDPPC	0.03	0.21	0.88
URBAN	0.04	0.013	0.0047
BWS	0.5	0.11	0.00019
GDPPC × URBAN	-0.010	0.0034	0.0029
URBAN × BWS	-0.006	0.0018	0.00035

Note: See text for description of the regression models used. See Table 1 for explanation of abbreviations.

Table A5 | **Regression Coefficients for Projecting Domestic Withdrawals**

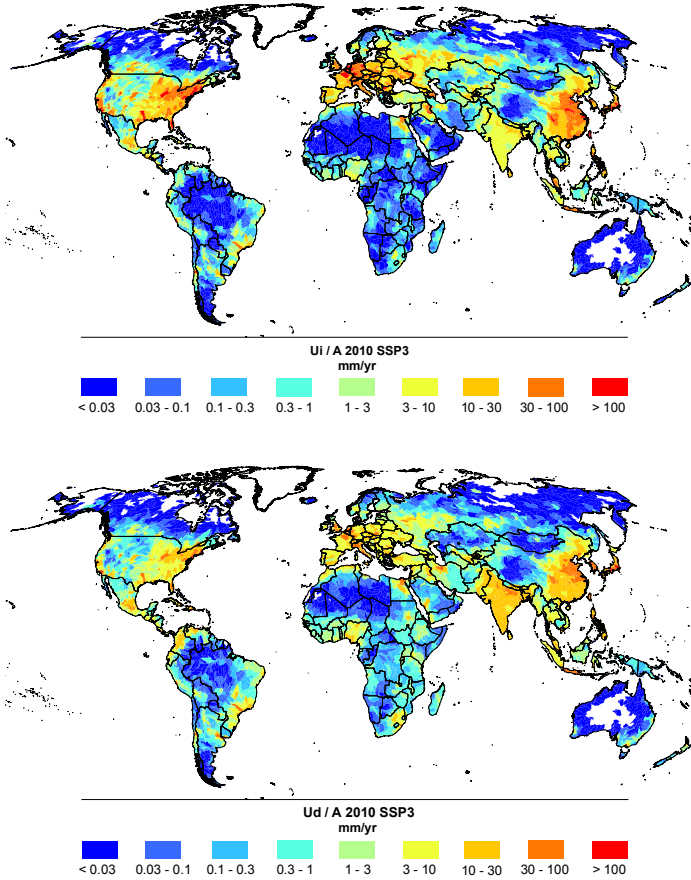
VARIABLE	VALUE	STD. ERROR	P-VALUE
AIC model			
Intercept	-0.6748	0.3112	0.031
GDPPC	0.5733	0.0880	< 0.001
URBAN	0.0336	0.0058	< 0.001
BWS	0.1606	0.0444	< 0.001
GDPPC × URBAN	-0.0069	0.0015	< 0.001
URBAN × BWS	-0.0013	0.0007	0.075
BIC model			
Intercept	-0.94	0.271	< 0.001
GDPPC	0.62	0.084	< 0.001
URBAN	0.04	0.005	< 0.001
BWS	0.09	0.012	< 0.001
GDPPC × URBAN	-0.01	0.001	< 0.001

Note: See text for description of the regression models used. See Table 1 for explanation of abbreviations.

Figure A6 | **Projected Industrial and Domestic Water Withdrawals for the Top Water Users in Each Sector, 2010**



Figure A7 | **Industrial Water Withdrawals and Domestic Water Withdrawals, 2010**



(cubic meters per 5 arc-minute cell)

A.5 Baseline correction and presentation of data

All data are available online at wri.org/aqueduct. In addition to displaying projections of change in each of the indicators, we also display the estimated value of each indicator in the target year. For the purposes of continuity with baseline indicators from Gassert et al.,¹⁵ we apply a simple linear correction to estimated future values for each of the indicators as follows. The projected rates of change for each indicator, as shown in the main text, are left uncorrected.

We computed corrected annual runoff ($R_{corr,t}$), consumptive water use ($Ct_{corr,t}$), total withdrawals ($Ut_{corr,t}$), and seasonal variability ($SV_{corr,t}$) for each of the future periods, t , as:

$$R_{corr,t} = R_{prj,t} + R_{base} - R_{prj,[1950-2010]}$$

$$Ct_{corr,t} = Ct_{prj,t} + Ct_{base} - Ct_{prj,[2010]}$$

$$Ut_{corr,t} = Ut_{prj,t} + Ut_{base} - Ut_{prj,[2010]}$$

$$SV_{corr,t} = SV_{prj,t} \frac{SV_{base}}{SV_{prj,[1950-2010]}}$$

where variables *prj* are from this study and variables *base* are from Gassert et al. Corrected total blue water and water stress are computed as above with the corrected input variables.

APPENDIX ENDNOTES

1. Detlef P. van Vuuren et al., “The Use of Scenarios as the Basis for Combined Assessment of Climate Change Mitigation and Adaptation,” *Global Environmental Change* 21, no. 2 (May 2011): 575–91, doi:10.1016/j.gloenvcha.2010.11.003.
2. Knutti and Sedláček, “Robustness and Uncertainties in the New CMIP5 Climate Model Projections.”
3. Todd Sanford et al., “The Climate Policy Narrative for a Dangerously Warming World,” *Nature Climate Change* 4, no. 3 (February 26, 2014): 164–66, doi:10.1038/nclimate2148.
4. Taylor, Stouffer, and Meehl, “An Overview of CMIP5 and the Experiment Design.”
5. O'Neill et al., “A New Scenario Framework for Climate Change Research: The Concept of Shared Socioeconomic Pathways.”
6. Brian C. O'Neill et al., “Meeting Report of the Workshop on The Nature and Use of New Socioeconomic Pathways for Climate Change Research, Boulder CO, November 2–4, 2011,” 2012, 1–37, <http://www.isp.ucar.edu/socio-economic-pathways>.
7. N. Hanasaki et al., “An Integrated Model for the Assessment of Global Water Resources—Part 1: Model Description and Input Meteorological Forcing,” *Hydrology and Earth System Sciences* 12 (2008): 1007–25, doi:10.5194/hess-12-1007-2008.
8. International Institute for Applied Systems Analysis (IIASA), “Shared Socioeconomic Pathways (SSP) Database (version 0.93).”
9. Earth System Grid Federation (ESGF), “Program for Climate Model Diagnosis and Interpretation (PCMDI),” n.d., <http://pcmdi9.llnl.gov/esgf-web-fe/>.
10. R. Alkama et al., “Detection of Global Runoff Changes: Results from Observations and CMIP5 Experiments,” *Hydrology and Earth System Sciences Discussions* 10 (2013): 2117–40, doi:10.5194/hessd-10-2117-2013.
11. Aiguo Dai et al., “Changes in Continental Freshwater Discharge from 1948 to 2004,” *Journal of Climate* 22, no. 10 (May 1, 2009): 2773–92, doi:10.1175/2008JCLI2592.1.
12. Rui and Beaudoin, *README Document for Global Land Data Assimilation System Version 2 (GLDAS-2) Products (Vol. 2)*.
13. National Center for Atmospheric Research (NCAR), “NCAR Command Language,” 2013, <http://www.ncl.ucar.edu>.
14. Open Source Geospatial Foundation, “GDAL—Geospatial Data Abstraction Library, Version 1.9.2,” 2013, <http://gdal.org>.
15. Gassert et al., *Aqueduct Global Maps 2.1: Constructing Decision-Relevant Global Water Risk Indicators*.

ACKNOWLEDGMENTS

This publication was made possible thanks to the ongoing support of the World Resources Institute Food, Forests, and Water Program and the Aqueduct Alliance. The authors would like to thank the following people for providing invaluable insight and assistance: Thomas Parris, Tianyi Luo, Andrew Maddocks, Tien Shiao, Betsy Otto, Charles Iceland, and Paul Reig, as well as Naota Hanasaki, Ramdane Alkama, and Kathleen Neumann for sharing their data. For their guidance and feedback during the development of the Aqueduct Water Stress Projections, the authors would also like to thank:

Adam Schlosser, Massachusetts Institute of Technology
Bruce Stewart, World Meteorological Organization
Mark Tadross, United Nations Development Programme
Yoshihide Wada, Utrecht University

ABOUT THE AUTHORS

Matt Luck is a research scientist at ISciences, L.L.C., where he develops and applies hydrological algorithms and models.

Contact: mluck@isciences.com

Matt Landis is a research scientist at ISciences, L.L.C., where he develops and applies hydrological algorithms and models.

Contact: landis@isciences.com

Francis Gassert is a research analyst with the Food, Forests, and Water Program at WRI, where he manages data collection and GIS analysis for the Aqueduct project.

Contact: fgassert@wri.org

ABOUT WRI

World Resources Institute is a global research organization that turns big ideas into action at the nexus of environment, economic opportunity and human well-being.

Our Challenge

Natural resources are at the foundation of economic opportunity and human well-being. But today, we are depleting Earth's resources at rates that are not sustainable, endangering economies and people's lives. People depend on clean water, fertile land, healthy forests, and a stable climate. Livable cities and clean energy are essential for a sustainable planet. We must address these urgent, global challenges this decade.

Our Vision

We envision an equitable and prosperous planet driven by the wise management of natural resources. We aspire to create a world where the actions of government, business, and communities combine to eliminate poverty and sustain the natural environment for all people.

Our Approach

COUNT IT

We start with data. We conduct independent research and draw on the latest technology to develop new insights and recommendations. Our rigorous analysis identifies risks, unveils opportunities, and informs smart strategies. We focus our efforts on influential and emerging economies where the future of sustainability will be determined.

CHANGE IT

We use our research to influence government policies, business strategies, and civil society action. We test projects with communities, companies, and government agencies to build a strong evidence base. Then, we work with partners to deliver change on the ground that alleviates poverty and strengthens society. We hold ourselves accountable to ensure our outcomes will be bold and enduring.

SCALE IT

We don't think small. Once tested, we work with partners to adopt and expand our efforts regionally and globally. We engage with decision-makers to carry out our ideas and elevate our impact. We measure success through government and business actions that improve people's lives and sustain a healthy environment.